

Document downloaded from:

<http://hdl.handle.net/10251/120459>

This paper must be cited as:

Aguado García, D.; Barat, R.; Bouzas Blanco, A.; Seco Torrecillas, A.; Ferrer, J. (2019). P-recovery in a pilot-scale struvite crystallisation reactor for source separated urine systems using seawater and magnesium chloride as magnesium sources. *The Science of The Total Environment*. 672:88-96. <https://doi.org/10.1016/j.scitotenv.2019.03.485>



The final publication is available at

<https://doi.org/10.1016/j.scitotenv.2019.03.485>

Copyright Elsevier

Additional Information

1 **P-recovery in a pilot-scale struvite crystallisation reactor for source separated urine systems**  
2 **using seawater and magnesium chloride as magnesium sources.**

3

4 D. Aguado\*, R. Barat\*, A. Bouzas\*\*, A. Seco\*\*, J. Ferrer\*

5

6 \*CALAGUA – Unidad Mixta UV-UPV, Institut Universitari d'Investigació d'Enginyeria de l'Aigua i Medi Ambient –  
7 IIAMA, Universitat Politècnica de València, Camí de Vera s/n, 46022 Valencia, Spain.

8 \*\*CALAGUA – Unidad Mixta UV-UPV, Departament d'Enginyeria Química, Universitat de València, Avinguda de la  
9 Universitat s/n, 46100 Burjassot, Valencia, Spain.

10

11 **Abstract**

12 Practical recovery of a non-renewable nutrient, such as phosphorus (P), is essential to support modern agriculture in the  
13 near future. The high P content of urine, makes it an attractive source for practicing the recovery of this crucial nutrient.  
14 This paper presents the experimental results at pilot-plant scale of struvite crystallization from a source-separated urine  
15 stream using two different magnesium sources, namely magnesium chloride and seawater. The latter was chosen as  
16 sustainable option to perform P-recovery in coastal areas. Real seawater was used to assess in a more realistic way its  
17 efficiency to precipitate P as struvite, since its composition (with noticeable concentration of ions such as  $\text{Ca}^{2+}$ ,  $\text{SO}_4^{2-}$ ,  
18  $\text{Na}^+$ ,...) could lead to the formation of impurities and other precipitates. 0.99 grams of struvite were obtained per litre of  
19 urine irrespective of the operational conditions tested. In all tested conditions, precipitation efficiencies exceeded 90%  
20 and recovery efficiencies were higher than 87%, with an average struvite crystal size higher than 110  $\mu\text{m}$  (and up to 320  
21  $\mu\text{m}$ , depending on the experimental conditions) in the harvested struvite samples. Almost pure struvite was obtained  
22 when  $\text{MgCl}_2$  was used as precipitant, while amorphous calcium phosphate and other impurities appeared in the  
23 precipitates using seawater as magnesium source. However, the lower settling velocity of the amorphous precipitates in  
24 comparison with the struvite precipitates suggest that their separation at industrial scale could be relatively  
25 straightforward.

26

27 **Keywords** phosphorus recovery; struvite; urine; crystallization; seawater

28

29

30

## 31 **1. INTRODUCTION**

32 Spontaneous precipitation of P-precipitates on internal pipe walls and surface equipment of  
33 Wastewater Treatment Plants (WWTPs) is possible due to the phosphorus (P) content in wastewater  
34 (Ohlinger *et al.*, 1998; Barat *et al.*, 2009). This unexpected precipitation can lead to operational  
35 problems such as scale formation, which results in reduced diameter or even blocked pipelines and  
36 higher operational costs in the sludge handling facilities (Neethiling and Benisch, 2004). Moreover,  
37 when this nutrient is not removed from wastewater at WWTPs, it reaches surface aquatic  
38 ecosystems promoting eutrophication (an adverse response of the natural ecosystem characterized  
39 by an accelerated plant and algal growth) and algae blooms.

40

41 Phosphorus is a crucial and non-renewable nutrient essential for modern agriculture which requires  
42 extra P to maximize crop yields. The primary source for P-fertilisers is a limited resource,  
43 phosphate rocks, which current reserves are predicted to be exhausted within the next century  
44 (Cordell *et al.*, 2009, Li *et al.*, 2019). Although phosphorus can be removed from wastewaters by  
45 chemical precipitation and/or biological processes, the application of technologies for phosphorus  
46 recovery is of major interest due to its marketable value. Indeed, extensive research has been carried  
47 out in the last years and is expected to gather worldwide momentum in the near future (Birnhack *et*  
48 *al.*, 2015).

49

50 Approximately 17% of the total phosphorus in phosphate rock mined specifically for food  
51 production is lost in human excreta via wastewater, mainly in urine (Cordell, 2010). In this context,  
52 phosphate recovery from urine is an attractive choice, because phosphorus is present in inorganic  
53 form not bonded to the organic matter and urine represents only 1% of the total volume of  
54 wastewater while contains up to 50 % of the total phosphate load in municipal wastewaters  
55 (Wilsenach *et al.*, 2007; Mo and Zhang, 2013). Although different technologies can be used to  
56 recover phosphorus from urine, chemical precipitation in the form of minerals with direct

57 application to agriculture such as struvite ( $\text{MgNH}_4\text{PO}_4 \cdot 6\text{H}_2\text{O}$ ) is being intensively studied by the  
58 scientific community (Rahman *et al.*, 2011; Matynia *et al.*, 2013; Capdevielle *et al.*, 2013; Barbosa  
59 *et al.*, 2016). Magnesium ammonium phosphate (MAP or struvite) is a slow-release fertiliser that  
60 can be produced from urine, being a solid free from micro-pollutants (Ronteltap *et al.*, 2007). Its  
61 purity and low heavy metal content (Latifian *et al.*, 2012; Muhmood *et al.*, 2018) contribute to the  
62 marketable value of struvite. This ecological fertiliser can complement or partially replace  
63 conventional chemical fertilisers to satisfy modern agriculture P requirements.

64

65 Many works have already reported struvite recovery from wastewater. Some of them have focused  
66 on urine P-recovery as it has been considered one of the most suitable sources for practicing it due  
67 to its simplicity and economics (Mihelcic *et al.*, 2011; Dai *et al.*, 2014), but only a few of these  
68 studies have used seawater as low-cost magnesium source (Rubio-Rincon *et al.*, 2014). In addition,  
69 most of the researches published so far have performed *batch* recovery experiments at lab-scale  
70 (Zamora *et al.*, 2017) with P-rich solutions. The conclusions of these studies are difficult to scale-up  
71 in real applications (Li *et al.*, 2019) due to the short-term of the experiments and the complexity of  
72 the crystallisation process regarding to the crystalliser hydraulics, start-up procedure, solids  
73 harvesting, etc., thus, limiting a wide spread implementation in industry. Therefore, in this work the  
74 main research effort is to assess P-recovery at pilot-scale and long-term experiments using  $\text{MgCl}_2$   
75 and seawater as magnesium sources, so as to get valuable results directly applicable from a practical  
76 and engineering point of view. Although different sustainable magnesium sources are reported in  
77 literature (Kirinovic *et al.*, 2017; Kiani *et al.*, 2019), seawater was chosen as a low-cost and  
78 sustainable option to perform the P-recovery process in coastal areas. Real seawater from the  
79 Mediterranean Sea was used to assess its efficiency to precipitate P as struvite in a more realistic  
80 way, since its composition (with noticeable concentration of ions such as  $\text{Ca}^{2+}$ ,  $\text{SO}_4^{2-}$ ,  $\text{Na}^+$ ,...) could  
81 lead to the formation of impurities and other precipitates. Therefore, the major objective of this

82 work is to assess the efficiency of the pilot-scale crystallisation reactor to achieve phosphorus  
83 recovery producing high quality struvite in long-term experiments.

84

## 85 **2. MATERIALS AND METHODS**

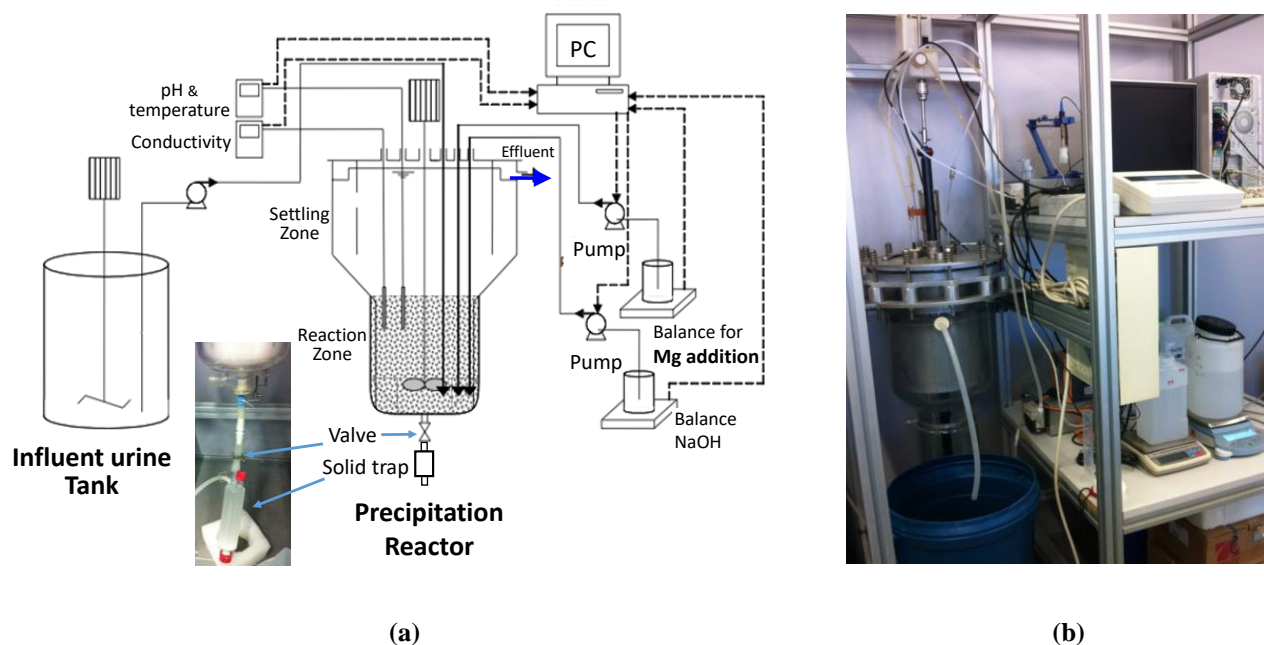
86

### 87 **2.1 Experimental set-up**

88

89 Figure 1 shows a scheme of the pilot plant used in this struvite precipitation research. As can be  
90 seen in Figure 1, the pilot plant consists of a glass stirred crystallisation reactor (20.55 L of volume)  
91 equipped with three pumps for influent (synthetic urine), magnesium source (seawater or  
92 magnesium chloride) and sodium hydroxide (for pH control) dosing through three independent  
93 stainless steel injection tubes, and two balances to monitor the magnesium and sodium hydroxide  
94 flows. The precipitation reactor is divided into two parts: the reaction zone (4.95 L in the bottom  
95 part), designed according to the typical dimensions of a perfectly mixed reactor and the top part  
96 which is the settling zone (15.60 L), that prevents fine particles from being lost with the effluent.  
97 Solid harvesting was carried out by settling. A solid trap was installed at the bottom part of the  
98 reaction zone (see snapshot detail in Figure 1a), and was connected to the reactor through a manual  
99 valve. This purge system allows the harvesting of the larger struvite crystals while the lower size  
100 solids remain growing within the reactor. When solid harvesting was desired, the trap was filled  
101 with the crystallisation effluent to avoid the hydrodynamic drag of the fluid velocity when the  
102 manual valve was opened. This allowed the lower size struvite crystals (with low settling velocity)  
103 remain in suspension within the reaction zone of the crystallisation reactor. Once opened the valve  
104 that connects the reaction zone with the solid trap, only the larger struvite crystals (able to settle)  
105 fell into the trap and were harvested from the reactor. When a prefixed height in the solid trap was  
106 achieved (the trap was roughly calibrated for different solid quantities in grams), the valve was  
107 closed and the trap emptied. Samples from the harvested mixture were used for further analytical

108 determinations such as solid size distribution, particles composition or weight of harvested struvite.  
 109 A detailed description of the pilot plant can be seen in Pastor *et al.* (2008a).  
 110  
 111



112 **Figure 1.** (a) Scheme of the struvite precipitation pilot-plant with snapshot of the purge system for struvite crystal  
 113 harvesting (b) Picture of the whole pilot-plant used in this study.

114

## 115 2.2 Substrates

116

117 The crystallisation reactor was fed with synthetic urine that reproduce the ions concentrations  
 118 observed in urine stored during three days (Table 1) and diluted according to the typical dilution  
 119 rate 1:4 in no-mix toilets (Udert *et al.*, 2003). Previous studies have shown that after three days of  
 120 hydrolysis, urine has suitable characteristics to recover P by crystallisation (pH around 8, and N/P  
 121 molar ratio above the stoichiometric requirements). Since the longer the storage time, the larger the  
 122 storage tank required, a three-day storage time was selected for urine. The reagents used to prepare  
 123 the synthetic substrate were:  $\text{CaCl}_2 \cdot 2\text{H}_2\text{O}$ ,  $\text{MgCl}_2 \cdot 6\text{H}_2\text{O}$ ,  $\text{NaCl}$ ,  $\text{Na}_2\text{SO}_4$ ,  $\text{Na}_3\text{C}_6\text{H}_5\text{O}_7 \cdot 2\text{H}_2\text{O}$ ,  
 124  $\text{KH}_2\text{PO}_4$ ,  $\text{KCl}$ ,  $\text{NH}_4\text{Cl}$  and  $(\text{NH}_4)_2\text{CO}_2$ .

125

126 **Table 1.** Synthetic urine used in the experimentation. Compounds concentration is expressed in mg/L

Na <sup>+</sup>	Cl <sup>-</sup>	K <sup>+</sup>	SO <sub>4</sub> <sup>2-</sup>	Ca <sup>2+</sup>	Mg <sup>2+</sup>	PO <sub>4</sub> -P	NH <sub>4</sub> -N	pH
583	1037	320	617	56	13	196	378	8.0

127

128 Ammonium concentration in urine exceeds that required for complete phosphorus recovery, but  
129 magnesium content is insufficient. The magnesium ions needed for struvite formation were  
130 provided by magnesium chloride (MgCl<sub>2</sub>·6H<sub>2</sub>O) solution in the first set of experiments, and by  
131 Mediterranean seawater in the second set, since it is a low-cost sustainable option in coastal areas.  
132 Magnesium chloride was chosen because it allows obtaining the desired Mg/P molar ratio without  
133 modifying the pH. The reagent solution used in the experiments was adjusted to 1300 mg Mg<sup>2+</sup>/L  
134 (similar concentration of Mg found in seawater) making it possible a direct comparison with the  
135 results obtained with seawater as magnesium source. Along each experiment the pH was adjusted  
136 with a sodium hydroxide (NaOH) solution (0.3 M) added on demand through a peristaltic pump.

137

### 138 **2.3 Analytical Methods**

139

140 PO<sub>4</sub>-P, NH<sub>4</sub>-N, NO<sub>3</sub>-N, NO<sub>2</sub>-N total phosphorus (TP), total nitrogen (TN) and chemical oxygen  
141 demand (COD) analysis were performed in accordance with Standard Methods (APHA, 2012).  
142 Total phosphorus of the crystallisation effluent was analysed acidifying the samples to pH around 2-  
143 3, ensuring that all phosphorus became soluble, and then analysed as PO<sub>4</sub>-P. Soluble calcium,  
144 magnesium, potassium, sodium, chloride and sulphate were analysed by ion chromatography  
145 (Metrohm IC). Alkalinity was measured by titration using the method proposed by Moosbrugger *et*  
146 *al.* (1992). For the analysis of soluble components, samples were previously filtered through 0.45  
147 µm filters.

148

149 The precipitated solids obtained in the crystalliser were recovered from the reaction zone and were  
150 air dried at room temperature. Scanning Electron Microscopy (SEM) coupled to energy-dispersive  
151 X-ray spectroscopy (EDS) was used to determine the morphology and composition of the harvested  
152 crystals as well as the main ions spatial distribution. The presence of P, N, Mg, Ca and K were  
153 searched by EDS microanalysis by means of a XL-30 ESEM (Philips, Eindhoven, Netherlands).  
154 Struvite samples were attached to the SEM stub using silver lacquer. Then, the SEM stub with the  
155 sample was introduced into the XL-30 and the pressure was diminished until  $10^{-5}$  bar. After that, the  
156 sample surface was visualised and an area was selected for the microanalysis. The spot-size value  
157 was modified until a Dead Time (DT) around 30% was achieved.

158

159 Crystal size distribution was determined by Malvern particle-sizer (Mastersizer 3000; measuring  
160 range 100 nm – 3 mm). The central value of the distribution was used as representative size and its  
161 evolution along the experiments is presented in the results and discussion section.

162

163 Finally, the solids were analysed by X-Ray Powder Diffraction (XRD) in order to check whether  
164 struvite crystals were formed. The equipment used for X-ray analyses was a D8 Avance A25  
165 powder diffractometer (Bruker, Karlsruhe, Germany). About 0.01 g of sample were placed in a  
166 sample holder and then into the X-ray chamber at 1200 °C. A scanning step of 0.02 ° and a pass of  
167 0.02 s were fixed as working constants.

168

## 169 **2.4 Experimental procedure**

170

171 The experimental work was divided into two sets of long-term experiments (see Table 2 for  
172 experimental conditions) carried out using the synthetic urine defined in Table 1. The shortest  
173 experiment lasted 15 days while the longest experiment 34 days, thus making it possible to  
174 reproduce the long-term real operation of the crystalliser, studying relevant engineering issues for



175 practical application such as the stability of the process or the evolution of the crystals size. In the  
 176 first set of experiments, magnesium chloride ( $\text{MgCl}_2 \cdot 6\text{H}_2\text{O}$ ) was used as magnesium source, while  
 177 in the second set, Mediterranean Seawater provided the magnesium ions required for the struvite  
 178 precipitation. In all the experiments, the crystalliser was operated in continuous mode for the liquid  
 179 phase and in batch-wise mode for the solid phase.

180

181 **Table 2.** Experimental conditions of the seven experiments.

Set	Experiment	Mg source	Duration (d)	pH	Molar ratio (Mg/P)	HRT (h)
Set 1	Exp 1	$\text{MgCl}_2 \cdot 6\text{H}_2\text{O}$	27	8.8	1	4.35
	Exp 2		30			3.26/2.45*
	Exp 3		15			1.5
	Exp 4		17			1/0.5*
Set 2	Exp 5	Seawater	34	8.8	1	4.35
	Exp 6		21			
	Exp 7		30			

182 \* Within these experiments different hydraulic retention times (HRT) were tested (i.e., a different HRT was applied without starting a  
 183 new experiment).

184

185 Synthetic urine fed to the crystallisation reactor had a high pH but not enough to counteract the pH  
 186 decrease caused by the crystallisation process. According to Pastor *et al.*, (2008a) the pH value in  
 187 the crystallisation reactor is an important parameter to achieve suitable efficiencies, and are  
 188 maximized at pH=8.8. Therefore, all experiments were performed at this pH value, and this  
 189 parameter was controlled at the desired set-point adding NaOH on demand using a fuzzy-logic  
 190 control algorithm (Chanona *et al.*, 2006).

191

192 In each experiment, samples from the effluent were taken on a daily basis to measure pH,  
193 conductivity, alkalinity, total phosphorus, orthophosphate, ammonium, magnesium, calcium,  
194 potassium, chloride and sodium.

195

196 Two types of efficiencies were calculated to evaluate the phosphorus precipitation process:  
197 precipitation and recovery efficiencies. These efficiencies were calculated along each experiment  
198 with the average values obtained from the analyses. Precipitation efficiency (Eq. 1) represents the  
199 process efficiency from a thermodynamic point of view since with enough residence time,  
200 supersaturation can be almost completely consumed. Recovery efficiency (Eq. 2) takes into account  
201 both precipitation and crystal growth efficiencies. It is calculated as the percentage of the total  
202 phosphorus entering the crystallisation reactor that is not lost with the effluent (i.e., total  
203 phosphorus entering the reactor minus total phosphorus leaving the reactor). The difference  
204 between both efficiencies corresponds to the fine crystals that are lost with the effluent of the  
205 crystallisation reactor.

206

$$\text{Precipitation efficiency} = \frac{(PO_4 - P_{influent}) - (PO_4 - P_{effluent})}{PO_4 - P_{influent}} \cdot 100\% \quad \text{Eq. 1}$$

$$\text{Recovery efficiency} = \frac{TP_{influent} - TP_{effluent}}{TP_{influent}} \cdot 100\% \quad \text{Eq. 2}$$

207

### 208 3. RESULTS AND DISCUSSION

209

210 All the experiments in the pilot-plant crystallisation reactor were performed at pH=8.8, Mg/P molar  
211 ratio of 1, 400 rpm stirring rate and started-up with 80 grams of struvite crystals as initial seed to  
212 avoid fouling on the reactor walls. These initial conditions were determined in a set of preliminary  
213 experiments. In these preliminary experiments, different strategies to avoid fouling on the reactor

214 walls were tested, such as starting-up the experiment with low pH and low Mg/P ratio and gradually  
215 increase them until reaching the desired set-points for the experiment, or using different grams of  
216 struvite crystals as initial seed of the experiment. Figure 2 shows some pictures from these  
217 preliminary experiments. Fouling on the internal reactor walls of the reaction zone as well as on the  
218 metallic stirrer occurred during the start-up of the experiment seeded with 9 grams of struvite  
219 crystals (see Figures 2a, 2b). The fouling was consequence of high supersaturation of the reactants  
220 concentration (i.e.,  $\text{NH}_4\text{-N}$ ,  $\text{PO}_4\text{-P}$ ,  $\text{Mg}^{2+}$ ) in the reaction zone, promoting primary nucleation  
221 instead of crystal growth. Conversely, no fouling occurred in the experiments started-up with 80  
222 grams of struvite crystals as initial seed (see Figure 2c). The main conclusion of these preliminary  
223 experiments was that with enough struvite seed in the reactor, no fouling occurred making it  
224 unnecessary taking any other measure to avoid supersaturation conditions.

225



(a)

(b)

(c)

226 **Figure 2.** Pictures of some preliminary experiments: (a) Fouling on the internal reactor walls of the reaction zone  
227 during the start-up of an experiment seeded with 9 grams of struvite crystals after 3 days of operation (b) fouling on the  
228 metallic stirrer (same experiment as before) (c) reaction zone during the start-up of an experiment seeded with 80 grams  
229 of struvite crystals after 30 days of operation.

230

231

232

### 233 3.1 Experiments with MgCl<sub>2</sub> as Mg source

234

235 Figure 3 shows the temporal evolution of different monitored parameters in the struvite  
236 precipitation experiments that used MgCl<sub>2</sub> as precipitant: solid concentration in the reaction zone,  
237 size of the solid crystals from the reaction zone (RZ Size) and from the harvest zone (HZ Size), as  
238 well as the precipitation and recovery efficiencies along each experiment. As can be seen in Figure  
239 3a, after starting the first experiment (HRT=4.35 h), the concentration of solids in the reaction zone  
240 increased, precipitation and recovery efficiencies quickly achieved high values (exceeding 90% at  
241 day 7), and both efficiencies began to separate around day 12, reflecting the presence of fine solids  
242 that were lost with the effluent. This difference in precipitation and recovery efficiencies was due to  
243 operating problems with the magnesium dosage (caused by scale deposits inside the magnesium  
244 injection pipeline), and when solved (with acid cleaning and regular maintenance of the injection  
245 pipeline) both efficiencies tended to converge again (day 16). Crystal harvesting from the  
246 precipitation reactor (at days 16, 21 and 26) allowed the solid concentration in the reaction zone to  
247 be relatively steady, enabling suitable continuous operation of the crystallisation process.

248

249 Struvite crystal size in the reaction zone followed a similar pattern to the solid concentration  
250 evolution, which can be clearly observed in Figure 3a. From day 3 onwards the crystal size was  
251 clearly visible at bare eye (> 100 µm), and a noticeable difference in size can be observed between  
252 the struvite crystals from the reaction zone (RZ Size) and the harvest zone (HZ Size). This size  
253 dissimilarity is consequence of the harvesting system implemented, which included a solid trap in  
254 the lower part of the reaction zone (see Figure 1a), acting as a settler, which was connected to the  
255 reactor through a manual valve. This purge system allowed the harvesting of the larger struvite  
256 crystals while keeping the lower size solids in suspension inside the reactor and letting them grow.

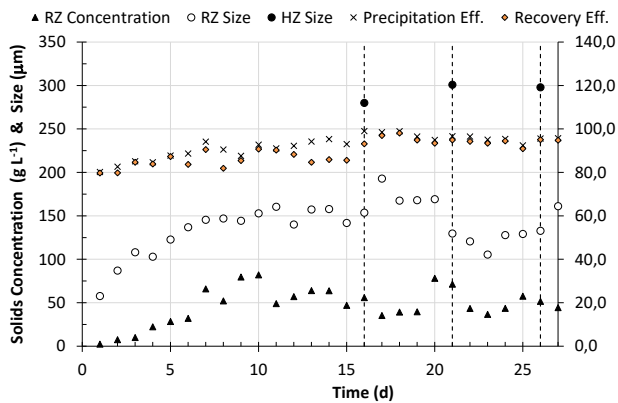
257

258

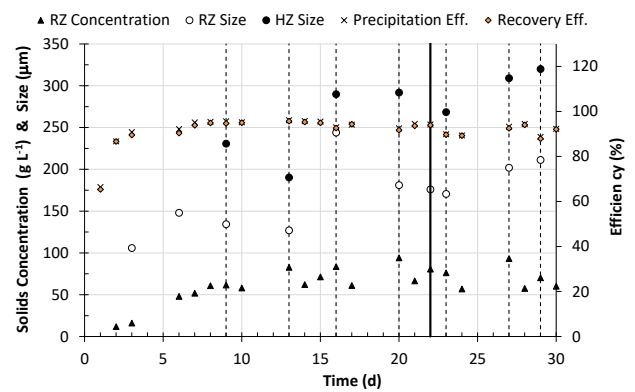
259 The experimentation results evidenced that the crystallisation process can continuously operate with  
 260 hydraulic retention times (HRT) as low as 0.5 hours (Figure 3) achieving consistently phosphorus  
 261 precipitation and recovery efficiencies higher than 90%. The lower the HRT the higher struvite  
 262 harvesting to maintain a steady solid concentration in the reaction zone (from 190 g of struvite per  
 263 week at 4.35 hours to 1610 g per week at 0.5 hours; resulting in 0.99 g of struvite per litre of urine).  
 264 The main effect of lowering the HRT was observed on the average size of the harvested struvite  
 265 crystals (and mainly on the size of solids from the harvest zone) that decreased from around 300  $\mu\text{m}$   
 266 at 4.35 hours to less than 200  $\mu\text{m}$  at 0.5 hours. To enable visual correlation patterns between the  
 267 different measured parameters and the HRT (i.e., the operational variable modified in each  
 268 experiment), a scatterplot of all variables is shown in Figure 4. As can be seen in Figure 4a no  
 269 significant difference existed in the recovery efficiencies achieved at the different HRT tested  
 270 (independently of the solid concentration in the reaction zone, which is influenced by the crystal  
 271 solid harvesting), while the harvested struvite crystals reduced in size as the HRT decreased for  
 272 values lower than 2.45 hours (Figure 4b). At higher HRT values the size of harvested struvite  
 273 crystals remained similar. An analogous correlation pattern was observed for the struvite crystals  
 274 from the reaction zone.

275

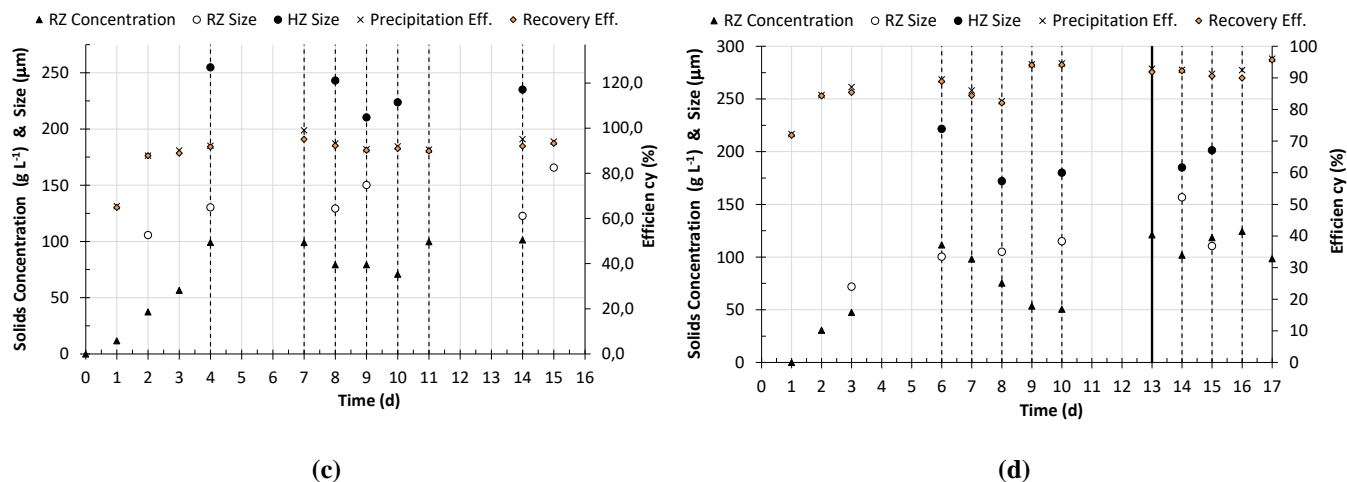
276



(a)

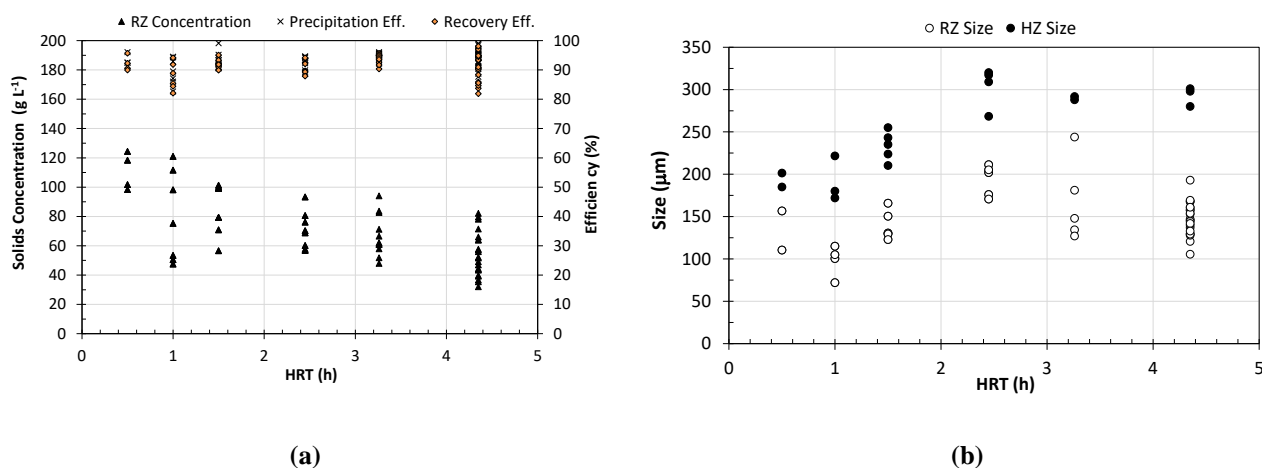


(b)



277 **Figure 3.** Time course evolution of recorded parameters in the struvite precipitation experiments that used  $MgCl_2$  as  
 278 precipitant: (a) Experiment 1 – HRT=4.35 h (b) Experiment 2 – HRT =3.26 h and 2.45 h (c) Experiment 3 – HRT =1.5  
 279 h (d) Experiment 4 – HRT=1 h and 0.5 h. Parameters shown: Solid concentration in the reaction zone (RZ  
 280 Concentration), size of the solid crystals from the reaction zone (RZ Size), size of the crystals from the harvest zone  
 281 (HZ Size), precipitation efficiency and recovery efficiency. Days when struvite crystals were harvested from the  
 282 crystallisation reactor are labelled with a vertical dashed line. Each vertical solid line signals a change in the HRT  
 283 within the experiment (i.e., a different HRT was applied without starting a new experiment).

284  
285  
286



287 **Figure 4.** Hydraulic retention time versus recorded parameters in the struvite precipitation experiments that used  $MgCl_2$   
 288 as precipitant. Parameters shown in: (a) Solid concentration in the reaction zone, precipitation efficiency and recovery  
 289 efficiency; (b) Size of the solid crystals from the reaction zone (RZ Size) and size of the crystals from the harvest zone  
 290 (HZ Size).

291

292

### 293 3.2 Experiments with seawater as Mg source

294

295 Another set of crystallisation experiments was performed using seawater instead of magnesium  
296 chloride as precipitant. As previously indicated, seawater was chosen as a low-cost and sustainable  
297 option to perform the P-recovery process in coastal areas. Real seawater from the Mediterranean  
298 Sea was used to assess its efficiency to precipitate P as struvite in a more realistic way. Average  
299 composition of the seawater used for the crystallisation experiments is shown in Table 3. As can be  
300 seen in this table, seawater presents noticeable concentration of ions such as  $\text{Ca}^{2+}$ ,  $\text{SO}_4^{2-}$ ,  $\text{Na}^+$ ,...  
301 which could lead to the formation of impurities and other precipitates.

302

303 **Table 3.** Average seawater composition of the samples from the Mediterranean Sea used in the experimentation.  
304 Average values and Standard Deviation of 70 samples. Compounds concentration is expressed in mg/L, Alkalinity as  
305  $\text{mgCaCO}_3/\text{L}$  and Conductivity in  $\text{mS}/\text{cm}$ .

$\text{Na}^+$	$\text{Cl}^-$	$\text{K}^+$	$\text{SO}_4^{2-}$	$\text{Ca}^{2+}$	$\text{Mg}^{2+}$	$\text{PO}_4\text{-P}$	$\text{NH}_4\text{-N}$	$\text{NO}_2\text{-N}$	$\text{NO}_3\text{-N}$	Alkalinity	Conductivity	pH
10947	20639	468.7	3022.3	441.6	1322	0.025	0.34	0	0.04	102.7	53	7.90
$\pm 1185$	$\pm 2168$	$\pm 34.6$	$\pm 345.7$	$\pm 52.9$	$\pm 124.4$	$\pm 0.005$	$\pm 0.12$		$\pm 0.02$	$\pm 5.1$	$\pm 6$	$\pm 0.04$

306

307 Figure 5 shows the temporal evolution of different monitored parameters in the struvite  
308 precipitation experiments that used Mediterranean Seawater as magnesium source: solid  
309 concentration in the reaction zone (RZ Concentration), size of the solid crystals from the reaction  
310 zone (RZ Size) and from the harvest zone (HZ Size), as well as the precipitation and recovery  
311 efficiencies. All experiments were carried out at the highest HRT tested in the  $\text{MgCl}_2$  set of  
312 experiments (4.35 h).

313

314 As can be seen in Figure 5, precipitation efficiency with seawater was consistently over 90%, while  
315 the recovery efficiency was close to 90% (88.9% on average). Although general patterns and

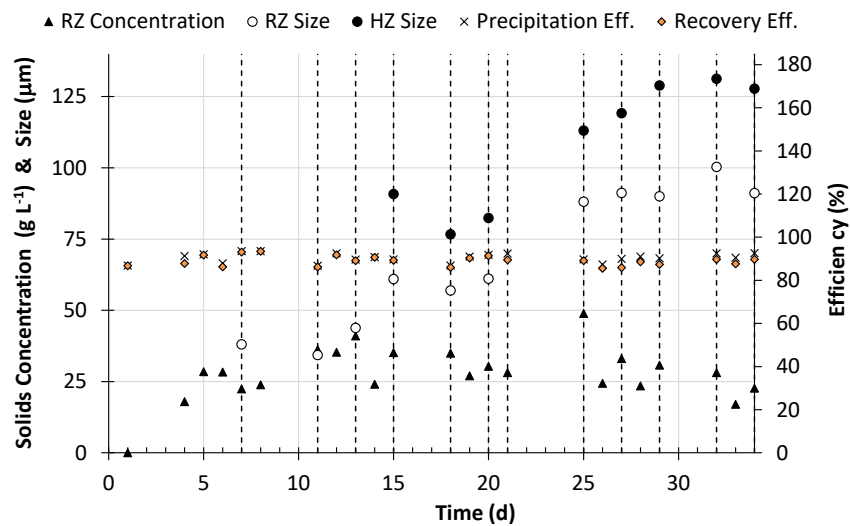
316 behaviour with seawater were similar to the results of  $MgCl_2$  as precipitant (compare Figure 3a with  
317 5a), remarkable differences can be observed. The main difference between both precipitants is the  
318 struvite crystal solid size, which is in this case (Mediterranean Seawater as magnesium source)  
319 clearly smaller. Both crystal sizes were smaller, the solids from the reaction zone (90  $\mu m$  vs 150  
320  $\mu m$ ) and the harvested solids (125  $\mu m$  vs 300  $\mu m$ ). This reduction in the crystal solid size can be  
321 due to the higher concentration of calcium in the seawater. Several authors (Le Corre *et al.*, 2005;  
322 Wang *et al.*, 2005; Pastor *et al.*, 2008b) have reported the influence of calcium concentration on  
323 struvite formation, evidencing a reduction in crystal size and a higher presence of amorphous form  
324 at the expense of the typical cuboid crystals of struvite as the concentration of calcium increased. Le  
325 Corre *et al.* (2005) indicated that Ca/Mg molar ratio of 0.5 inhibited struvite growth, generating  
326 amorphous calcium phosphate precipitated on struvite surface; and Ca/Mg molar ratio above 1 gave  
327 rise to the formation of an amorphous precipitate rather than crystalline struvite. Pastor *et al.*  
328 (2008b) observed a lower struvite formation at Ca/Mg molar ratio of 1.6. Gao *et al.* (2018) observed  
329 that the increase of  $Ca^{2+}$  concentration influenced potassium struvite crystallization from urine due  
330 to the formation of calcium phosphate. Li *et al.* (2016) also observed that a calcium concentration  
331 with a calcium to magnesium ratio of less than one helps increase the particle size of the crystals  
332 without negatively impacting on the product purity. Thus, the particle size can potentially be used to  
333 infer the product purity. However, these effects are less potent at a high ammonia nitrogen  
334 concentration, which diminishes the negative impact of calcium. In this work, the Ca/Mg ratio was  
335 0.2 and 0.4 for the experiments using magnesium chloride and seawater, respectively. The Ca/Mg  
336 ratio slightly increased when seawater was used, which could favour the reduction of the crystal  
337 solid size observed in these experiments.

338

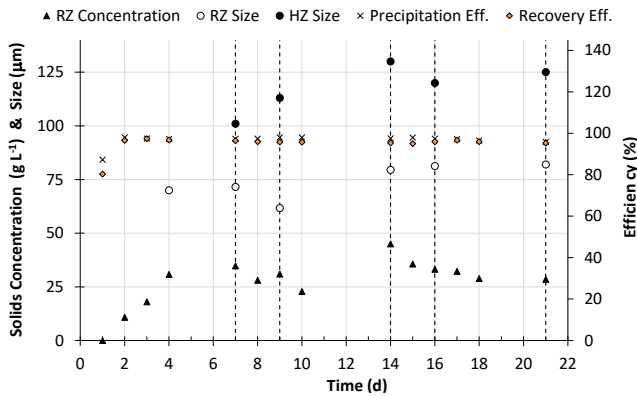
339 Another difference in the experiments with seawater as magnesium source is the presence of  
340 impurities and amorphous precipitates. Although the Ca/Mg molar ratio increase observed in  
341 seawater experiments was not high enough to inhibit struvite formation, this increase could help to



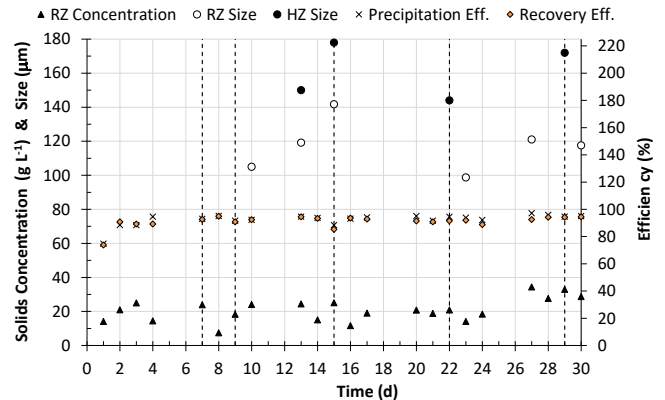
342 give rise to the formation of this amorphous precipitate. Figure 6 shows their presence in the solid  
 343 trap. However, a clear difference was observed in the settling velocity of the struvite crystal solids  
 344 and the amorphous precipitates, which as can be seen in Figure 6, rested as a layer on top of the  
 345 struvite. This clear difference in the two layers formed naturally within the solid trap suggest that  
 346 the separation of the amorphous matter from the struvite crystals at industrial scale could be  
 347 possible and relatively straightforward. Anyway, specific experiments would be required to  
 348 evaluate the feasibility of this separation and its associated economic cost. In the remaining  
 349 experiments (Figures 5b and 5c), with durations up to 30 days, similar results were observed (high  
 350 precipitation and recovery efficiencies and the crystal size of the crystals from the harvest zone  
 351 noticeable higher than the solids from the reaction zone).



(a)

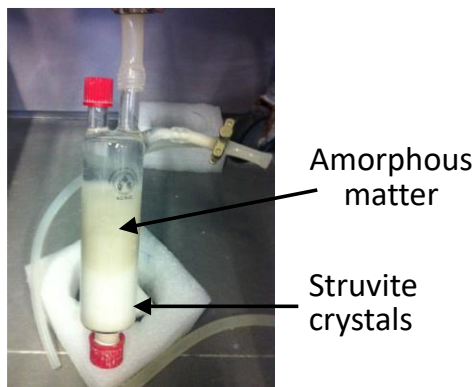


(b)



(c)

352 **Figure 5.** Time course evolution of recorded parameters in the struvite precipitation experiments that used  
353 Mediterranean Seawater as magnesium source: (a) Experiment 5 (b) Experiment 6 (c) Experiment 7. All experiments  
354 were performed at 4.35 hours of HRT. Parameters shown: Solid concentration in the reaction zone (RZ Concentration),  
355 crystals solid size in the reaction zone (RZ Size), crystals solid size of the harvest zone (HZ Size), precipitation  
356 efficiency and recovery efficiency. Days when struvite crystals were harvested from the crystallisation reactor are  
357 labelled with a vertical dashed line.  
358  
359

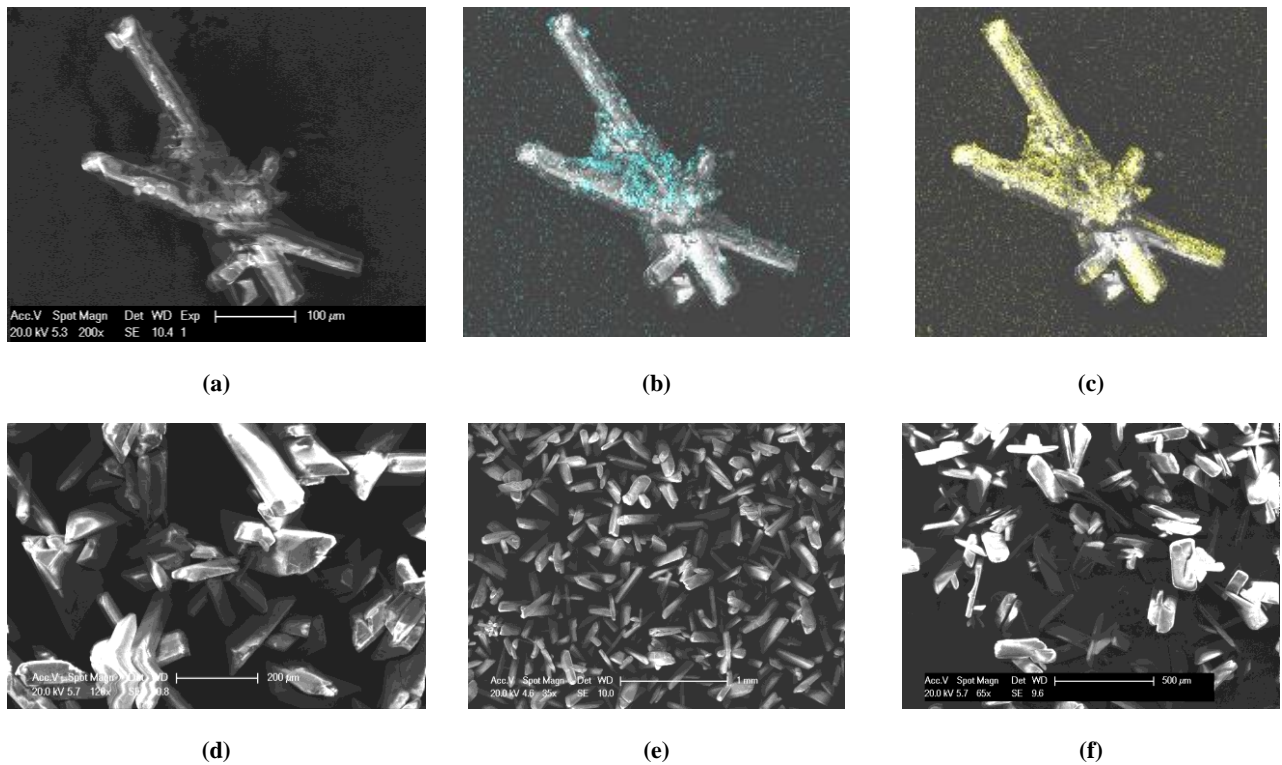


360 **Figure 6.** Picture of the solid trap with harvested solids from the crystallisation reactor at the end of the Experiment 5.  
361  
362 Several SEM images of the struvite precipitates from Experiment 5 carried out using seawater  
363 (upper part of the figure) and from Experiment 1 carried out using magnesium chloride (bottom  
364 part) as precipitants are shown in Figure 7. As can be seen in Figure 7a, the amorphous matter not  
365 only grew independently of struvite but also grew, covered and merged several orthorhombic  
366 struvite crystals. The calcium mapping (Figure 7b) clearly revealed the presence of calcium in this  
367 unstructured matter, which could probably be a mixture of calcite and amorphous calcium  
368 phosphate. In contrast, perfect cuboid crystals (Figures 7 d, 7e, 7f) were observed in the  
369 experiments where magnesium chloride was used as precipitant. Moreover, the qualitative  
370 composition (expressed as percentage of N, P, Mg and C) of the harvested crystals obtained by  
371 EDS, shown in Figure 8, revealed the presence of calcium in the precipitates formed in Experiment  
372 5 carried out using seawater.

373

374 Finally, to further understand the nature of the precipitates formed according to the magnesium  
375 source, XRD was used to determine the identity of the precipitates. The XRD pattern of the  
376 precipitates from experiments 1 and 5 are shown in Figure 9. The XRD patterns from samples  
377 obtained in the magnesium chloride experiments matched well with the peaks for pure struvite. In  
378 samples from seawater experiments, the diffractogram revealed some background noise, which  
379 indicated the presence of amorphous precipitate.

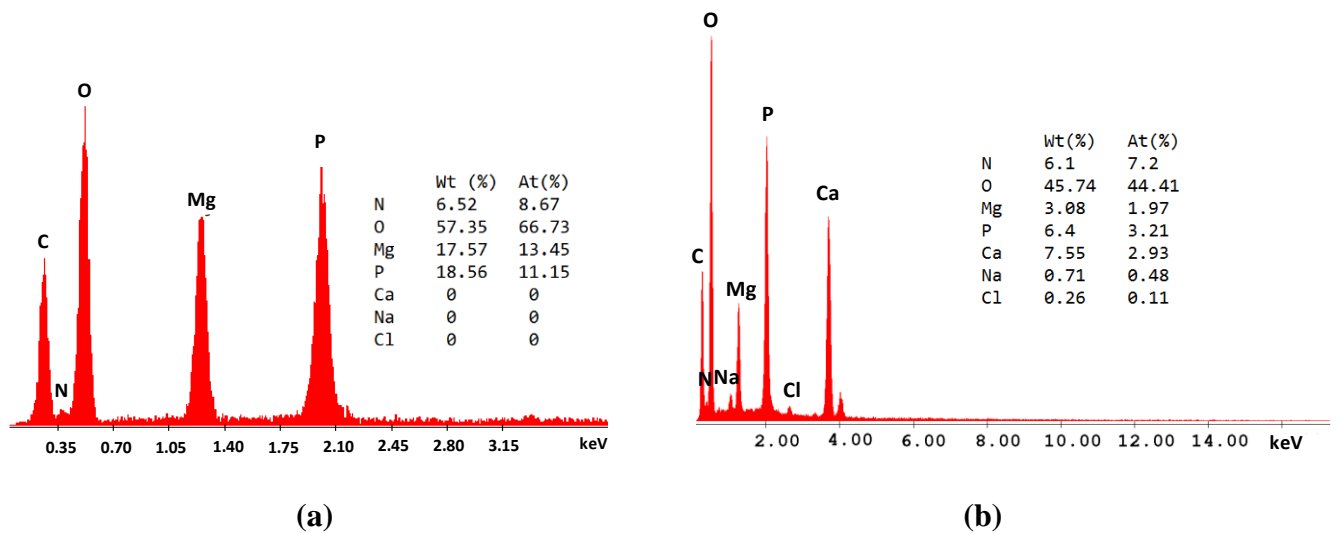
380



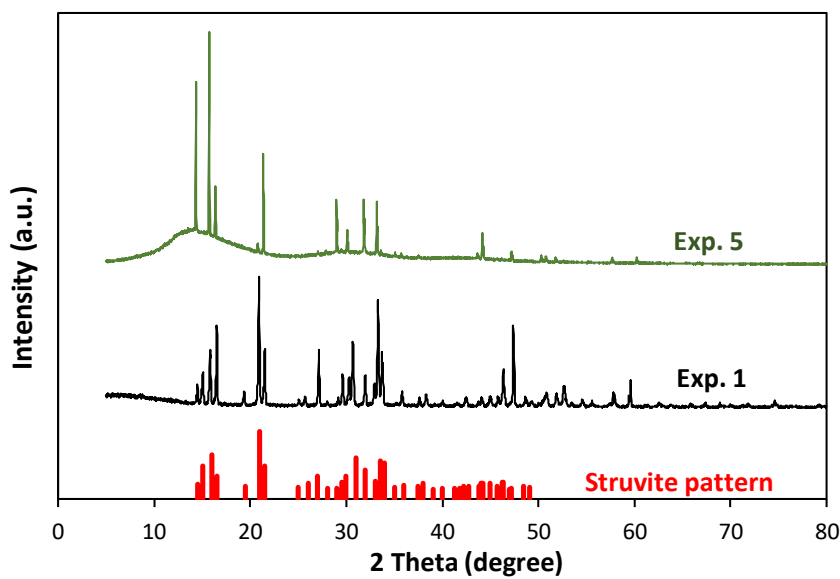
381 **Figure 7.** (a) SEM image of precipitates from the largest experiment carried out using seawater as magnesium source  
382 (Experiment 5) where an amorphous matter growing on several cuboid struvite crystals can be seen (b) Calcium  
383 mapping (c) Magnesium mapping. Bottom figures correspond to SEM images from experiments using MgCl<sub>2</sub> as  
384 precipitant (d,e) Experiment 1 – HRT=4,35 h (f) Experiment 2 – HRT=3,26 h.

385

386



387 **Figure 8.** X-ray microanalysis results for the struvite obtained from (a) Experiment 1 (using MgCl<sub>2</sub> as Mg source) and  
 388 (b) Experiment 5 (seawater as Mg source).  
 389



390 **Figure 9.** X-ray diffraction spectra of the precipitates from Experiment 1 (MgCl<sub>2</sub> was used as Mg source) and  
 391 Experiment 5 (seawater was used as Mg source), together with the standard struvite pattern.

392

#### 393 4. CONCLUSIONS

394 In this work, interesting experimental results at pilot-plant scale of struvite crystallization from  
 395 urine using magnesium chloride and Mediterranean Seawater as magnesium sources are presented,  
 396 thoroughly analysed and discussed. The main conclusions that can be drawn from this study are:

- 397
- Struvite crystallization in the pilot-scale reactor can be stable, with high P precipitation and
- 398 recovery efficiencies (exceeding 90% and 87%, respectively), achieving 0.99 grams of
- 399 struvite per litre of urine irrespective of the variations in the operational conditions.
- 400
- To avoid fouling on the reactor walls due to primary nucleation instead of crystal growth, it
- 401 is of paramount importance starting-up the process with enough struvite seed in the reactor.
- 402
- Crystal solids harvesting from the precipitation reactor allow the solid concentration in the
- 403 reaction zone to be relatively steady which is important to enable suitable continuous
- 404 operation of the crystallisation process.
- 405
- Settling allows the harvesting of the larger struvite crystals while the lower size solids
- 406 remain in the reactor making it possible its growth.
- 407
- The hydraulic retention time (HRT) does not affect the phosphorus precipitation and
- 408 recovery efficiencies, but as the HRT decreases the harvested struvite crystals tend to be
- 409 smaller.
- 410
- Larger struvite crystals were obtained (around 2-fold) using magnesium chloride instead of
- 411 seawater as magnesium source.
- 412
- Using seawater as low-cost magnesium source to perform P-recovery from urine in coastal
- 413 areas is feasible. High phosphorus precipitation and recovery efficiencies are possible (close
- 414 to 90%) with struvite crystals visible at bare eye ( $> 100 \mu\text{m}$ ).
- 415
- Impurities appeared in the P-precipitates using seawater as struvite magnesium source. The
- 416 lower settling velocity of the amorphous precipitates in comparison with the struvite
- 417 precipitates suggest that their separation at industrial scale could be relatively
- 418 straightforward.
- 419
- 420
- 421

## 422 **ACKNOWLEDGEMENTS**

423 This research work was possible thanks to FCC Aqualia participation in INNPRONTA 2011 IISIS  
424 IPT-20111023 project (partially funded by The Centre for Industrial Technological Development  
425 (CDTI) and supported by the Spanish Ministry of Economy and Competitiveness).

426

## 427 **REFERENCES**

- 428 APHA (2012). American Public Health Association/American Water Works Association/Water Environmental  
429 Federation. Standard Methods for the Examination of Water and Wastewater, 22nd edition, Washington DC, USA.
- 430 Barat R., Bouzas A., Martí N., Ferrer J., Seco A. (2009) Precipitation assessment in wastewater treatment plants  
431 operated for biological nutrient removal: A case study in Murcia, Spain. *Journal of Environmental Management*, 90  
432 (2), 850–857. doi:10.1016/j.jenvman.2008.02.001
- 433 Barbosa S.G., Peixoto L., Meulman B., Alves M.M., Pereira M.A. (2016) A design of experiments to assess  
434 phosphorous removal and crystal properties in struvite precipitation of source separated urine using different Mg  
435 sources. *Chemical Engineering Journal* 298, 146-153. doi: 10.1016/j.cej.2016.03.148
- 436 Birnhack L., Nir O., Telzhenski M., Lahav O. (2015). A new algorithm for design, operation and cost assessment of  
437 struvite ( $MgNH_4PO_4$ ) precipitation processes. *Environmental Technology* 36, (13-16) 1892-901. doi:  
438 10.1080/09593330.2015.1015455.
- 439 Capdevielle A., Sýkorová E., Biscans B., Béline F., Daumer ML. (2013). Optimization of struvite precipitation in  
440 synthetic biologically treated swine wastewater - determination of the optimal process parameters. *Journal of*  
441 *Hazardous Materials*, 244-245, 357-369. doi: 10.1016/j.jhazmat.2012.11.054
- 442 Chanona J., Pastor L., Borrás L., Seco A. (2006). Application of a fuzzy algorithm for pH control in a struvite  
443 crystallization reactor. *Water Science and Technology*. 53, 161–168. doi: 10.2166/wst.2006.418
- 444 Cordell D., Drangert J.-O., White S. (2009). The story of phosphorus: Global food security and food for thought. *Global*  
445 *Environmental Change*, 19 (2), 292–305. doi: 10.1016/j.gloenvcha.2008.10.009
- 446 Cordell D. (2010). The story of phosphorus: Sustainability implications of global phosphorus scarcity for food security.  
447 Doctoral Thesis. Collaborative Ph.D. between the Institute for Sustainable Futures, University of Technology,  
448 Sydney (UTS) & Department of Thematic Studies – Water and Environmental, Linköping University, Sweden .No.  
449 509. Linköping University Press, Linköping (ISBN: 9789173934404).

450 Dai J., Tang W.-T., Zheng Y.-S., Mackey H.R., Chui H.K., Van Loosdrecht M.C.M., Chen G.-H. (2014). An  
451 exploratory study on seawater-catalysed urine phosphorus recovery (SUPR). *Water Research* 66, 75–84.  
452 doi:10.1016/j.watres.2014.08.008

453 Kiani D., Sheng Y., Lu B., Barauskas D., Honer K, Jiang Z., Baltrusaitis J. (2019). Transient Struvite Formation during  
454 Stoichiometric (1:1)  $\text{NH}_4^+$  and  $\text{PO}_4^{3-}$  Adsorption/Reaction on Magnesium Oxide (MgO) Particles *ACS Sustainable*  
455 *Chemistry & Engineering* 7 (1), 1545-1556. doi: 10.1021/acssuschemeng.8b05318

456 Kirinovic E., Leichtfuss A. R., Navizaga C., Zhang H., Schuttlefield Christus J.D., Baltrusaitis J. (2017). Spectroscopic  
457 and Microscopic Identification of the Reaction Products and Intermediates during the Struvite ( $\text{MgNH}_4\text{PO}_4 \cdot 6\text{H}_2\text{O}$ )  
458 formation from Magnesium Oxide (MgO) and Magnesium Carbonate ( $\text{MgCO}_3$ ) Microparticles. *ACS Sustainable*  
459 *Chemistry & Engineering* 5 (2), 1567-1577. doi: 10.1021/acssuschemeng.6b02327

460 Latifian M., Liu J., Mattiasson B. (2012). Struvite-based fertilizer and its physical and chemical properties. *Environ*  
461 *Technol.* 33, 2691-2697. doi: 10.1080/09593330.2012.676073

462 Le Corre K.S., Valsami-Jones E., Hobbs P., Parsons S.A. (2005). Impact of calcium on struvite crystal size, shape and  
463 purity. *Journal of Crystal Growth*, 283: 514-522. doi:10.1016/j.jcrysro.2005.06.012

464 Li, B., Boiarkina, I., Young, B., Yu, W. (2016) Quantification and mitigation of the negative impact of calcium on  
465 struvite purity. *Advanced Powder Technology* 27, 2354–2362. doi: 10.1016/j.appt.2016.10.003

466 Li B., Boiarkina I., Yu W., Huang H.M., Munir T., Wang G.Q., Young B.R. (2019). Phosphorous recovery through  
467 struvite crystallization: Challenges for future design. *Science of The Total Environment* 648, 1244-1256. doi:  
468 10.1016/j.scitotenv.2018.07.166.

469 Matynia A., Wierzbowska B., Hutnik N., Mazienczuk A., Kozik A., Piotrowski K. (2013). Separation of struvite from  
470 mineral fertiliser industry wastewater. *Procedia Environmental Sciences* 18, 766–775. doi:  
471 10.1016/j.proenv.2013.04.103

472 Mihelcic J.R., Fry L.M., Shaw R. (2011). Global potential of phosphorus recovery from human urine and feces.  
473 *Chemosphere* 84 (6), 832–839. doi:10.1016/j.chemosphere.2011.02.046

474 Mo W., Zhang Q. (2013). Energy-nutrients-water nexus: Integrated resource recovery in municipal wastewater  
475 treatment plants. *Journal of Environmental Management* 127, 255-267. doi:10.1016/j.jenvman.2013.05.007

476 Moosbrugger RE., Wentzel MC, Ekama GA, Marais GVR. (1992) Simple Titration Procedure to Determine  $\text{H}_2\text{CO}_3$   
477 Alkalinity and Short Chain Fatty Acids in Aqueous Solutions Containing Known Concentrations of Ammonium,  
478 Phosphate and Sulphide Weak Acid/Bases. WRC Report W74.

479 Muhmood A., Wu S., Lu J., Ajmal Z., Luo H., Dong R. (2018). Nutrient recovery from anaerobically digested chicken  
480 slurry via struvite: Performance optimization and interactions with heavy metals and pathogens. *Science of The*  
481 *Total Environment* 635, 1-9. doi. 10.1016/j.scitotenv.2018.04.129

482 Neethling J.B., Benisch M. (2004). Struvite control through process and facility design as well as operation strategy.  
483 *Water Science and Technology*, 49 (2), 191-199.

484 Ohlinger K.N., Young T.M., Schroeder E.D. (1998). Predicting struvite formation in digestion. *Water Research*, 32,  
485 3607-3614. doi:10.1016/S0043-1354(98)00123-7

486 Pastor L., Mangin D., Barat R., Seco A. (2008a). A pilot-scale study of struvite precipitation in a stirred tank reactor:  
487 conditions influencing the process. *Bioresource Technology*. 99 (14), 6285–6291. doi:  
488 10.1016/j.biortech.2007.12.003

489 Pastor, L., Martí, N., Bouzas, A., Seco, A. (2008b). Sewage sludge management for phosphorus recovery as struvite in  
490 EBPR wastewater treatment plants. *Bioresour. Technol.* 99, 4817-4824. doi:10.1016/j.biortech.2007.09.054

491 Rahman M.M., Liu Y.H., Kwag, J.H., Ra C.S. (2011). Recovery of struvite from animal wastewater and its nutrient  
492 leaching loss in soil. *Journal of Hazardous Materials*, 186, 2026–2030. doi: 10.1016/j.jhazmat.2010.12.103

493 Ronteltap M., Maurer M., Gujer W. (2007). The behaviour of pharmaceuticals and heavy metals during struvite  
494 precipitation in urine. *Water Research* 41(9), 1859-1868. doi:10.1016/j.watres.2007.01.026

495 Rubio-Rincón F.J., Lopez-Vazquez C.M., Ronteltap M., Brdjanovic D. (2014). Seawater for phosphorus recovery from  
496 urine. *Desalination* 348, 49–56. doi:10.1016/j.desal.2014.06.005

497 Udert K.M., Larsen T.A., Gujer W. (2003). Biologically induced precipitation in urine-collecting systems. *Water*  
498 *Science and Technology*, 3 (3), 71–78. doi:10.2166/ws.2003.0010

499 Wang, J., Burken, J.G., Zhang, X., Surampalli, R. (2005). Engineered struvite precipitation: impacts of component-ion  
500 molar ratios. *J. Environ. Eng.* 131 (10), 1433–1440. doi.org/10.1016/j.watres.2016.03.032

501 Wilsenach J. A., Schuurbiens C.A.H., Van Loosdrecht, M.C.M. (2007). Phosphate and potassium recovery from source  
502 separated urine through struvite precipitation. *Water Research*, 41(2), 458-466. doi: 10.1016/j.watres.2006.10.014

503 Zamora P., Georgieva T., Salcedo I., Elzinga N., Kuntke P., Buisman C. J. (2017). Long-term operation of a pilot-scale  
504 reactor for phosphorus recovery as struvite from source-separated urine. *J. Chem. Technol. Biotechnol.* (92), 1035-  
505 1045. doi:10.1002/jctb.5079